A TRIDENT SCHOLAR PROJECT REPORT

NO. 226

"REACTION KINETICS OF Mo(a^7S_3, a^5D_4, a^5S_2) WITH CO_2, N_2O, SO_2, and NO "

UNITED STATES NAVAL ACADEMY
ANNAPOLIS, MARYLAND

REPORT DOCUMENTATION PAGE

Form Approved
OMB no. 0704-0188

1. AGENCY USE ONLY (Leave blank)	2. REPORT DATE	3. REPORT TYPE AND DATES COVERED
	9 May 1995	

4. TITLE AND SUBTITLE Reaction kinetics of Mo(a^7S_3, a^5D_4, a^5S_2) with CO_2, N_2O, SO_2, and NO

5. FUNDING NUMBERS

6. AUTHOR(S)

Robert H. Goodwin

7. PERFORMING ORGANIZATIONS NAME(S) AND ADDRESS(ES)

U.S. Naval Academy, Annapolis, MD

8. PERFORMING ORGANIZATION REPORT NUMBER USNA Trident report; no. 226 (1995)

9. SPONSORING/MONITORING AGENCY NAME(S) AND ADDRESS(ES)

10. SPONSORING/MONITORING AGENCY REPORT NUMBER

11. SUPPLEMENTARY NOTES

Accepted by the U.S. Trident Scholar Committee

12a. DISTRIBUTION/AVAILABILITY STATEMENT

This document has been approved for public release; its distribution is UNLIMITED.

12b. DISTRIBUTION CODE

13. ABSTRACT (Maximum 200 words) The gas phase reactivities of Mo(a^7S_3, a^5D_j, a^5S_2) with CONO, SO_2, and N_2O were measured under pseudo-first order conditions ([Mo]<<[oxidant]). The reactivities were measured over a temperature range of 297-600K and a pressure range of 20-300 Torr using an argon buffer. Mo atoms were produced by the photodissociation of $Mo(CO)_6$ or $MoCl_4$ and detected by laser-induced fluorescence. The concentration of Mo during its reaction with the oxidants was measured as a function of laser delay. This temporal behavior of Mo yields first order decay rate constants from which second order rate constants are determined. Biexponential behavior was noted in N_2O and CO_2 reacting with Mo(a^5S_2). It was found from the rate constants for the reactions of N_2O or CO_2 with Mo, that the Mo excited states with an s^1d^5 configuration react faster than states with an s^2d^4 configuration. This observation is attribute to the correlation of the s^1d^5 configuration to the ground state of MoO. N_2O and CO_2 reacted slowly with Mo in the ground a^7S_3 state due to spin prohibited behavior. NO reacting with the ground state showed a pressure dependent behavior. SO_2 reacted near the gas kinetic rate in all states observed.

14. SUBJECT TERMS	15. NUMBER OF PAGES
kinetics; laser photodissociation/laser induced fluorescence; transition metals; molybdenum	16. PRICE CODE

17. SECURITY CLASSIFICATION OF REPORT	18. SECURITY CLASSIFICATION OF THIS PAGE	19. SECURITY CLASSIFICATION OF ABSTRACT	20. LIMITATATION OF ABSTRACT
UNCLASSIFIED	UNCLASSIFIED	UNCLASSIFIED	UNCLASSIFIED

USNA Trident Scholar Project Report; no. 226 (1995)

"REACTION KINETICS OF Mo(a^7S_3, a^5D_4, a^5S_2) WITH CO_2, N_2O, SO_2, and NO "

by

Midshipman Robert H. Goodwin, Class of 1995
United States Naval Academy
Annapolis, Maryland

Certification of Adviser Approval
Associate Professor Mark L. Campbell
Department of Chemistry

Mark L. Campbell

9 May 1995

Acceptance for the Trident Scholar Committee

Professor Joyce E. Shade
Chair, Trident Scholar Committee

Joyce E. Shade

9 May 95

ABSTRACT

The gas phase reactivities of Mo(a^7S_3, a^5D_J, a^5S_2) with CO_2, NO, SO_2, and N_2O were measured under pseudo-first order conditions ([Mo] << [oxidant]). The reactivities were measured over a temperature range of 297-600K and a pressure range of 20-300 Torr using an argon buffer. Mo atoms were produced by the photodissociation of $Mo(CO)_6$ or $MoCl_4$ and detected by laser-induced fluorescence. The concentration of Mo during its reaction with the oxidants was measured as a function of laser delay. This temporal behavior of Mo yields first order decay rate constants from which second order rate constants are determined. Biexponential behavior was noted in N_2O and CO_2 reacting with Mo(a^5S_2).

It was found from the rate constants for the reactions of N_2O or CO_2 with Mo, that the Mo excited states with an s^1d^5 configuration react faster than states with an s^2d^4 configuration. This observation is attributed to the correlation of the s^1d^5 configuration to the ground state of MoO. N_2O and CO_2 reacted slowly with Mo in the ground a^7S_3 state due to spin prohibited behavior.

NO reacting with the ground state showed a pressure dependent behavior. SO_2 reacted near the gas kinetic rate in all states observed.

KEYWORDS

Kinetics

Laser Photodissociation / Laser Induced Fluorescence

Transition Metals

Molybdenum

TABLE OF CONTENTS

INDEX TO TABLES AND FIGURES

TABLES

FIGURES

I. Introduction

One of the primary goals in the study of chemistry is to understand the various factors which influence the rate and outcome of chemical reactions. Of primary importance in a reaction is the fundamental character of the reactants. This includes the influence of ionization potentials, electron affinities, and ground and low-lying excited electronic states on the chemical reaction.

Previous studies with Tungsten (W), Titanium (Ti), and Vanadium (V) have shown that transition metals in a s^1d^{n-1} configuration reacted faster than transition metals in a s^2d^{n-2} configuration where n is the number of valence electrons (see Table 1). These studies, however, compared a ground state with the s^2d^{n-2} configuration to an excited state with an s^1d^{n-1} configuration. Therefore, the differences in reactivities may possibly be due to energy differences between those states, and not electron configuration effects. Mo was chosen to be studied because it has a ground state configuration of s^1d^{n-1} (see Table 1). It can be hypothesized that the states with an s^1d^5 configuration [Mo (a^7S_3, a^5S_2)] will react faster than states with an s^2d^4 configuration [Mo (a^5D_4)] due to a correlation of the $\delta^2\sigma^1\pi^1$ configuration to the ground state of MoO ($^5\Pi$).

A. Transition Metal Chemistry

3	4	5	6	7	8	9	10	11	12
21 **Sc** $4s^2 3d^1$	22 **Ti** $4s^2 3d^2$	23 **V** $4s^2 3d^3$	24 **Cr** $4s^1 3d^5$	25 **Mn** $4s^2 3d^5$	26 **Fe** $4s^2 3d^6$	27 **Co** $4s^2 3d^7$	28 **Ni** $4s^2 3d^8$	29 **Cu** $4s^1 3d^{10}$	30 **Zn** $4s^2 3d^{10}$
39 **Y** $5s^2 4d^1$	40 **Zr** $5s^2 4d^2$	41 **Nb** $5s^1 4d^4$	42 **Mo** $5s^1 4d^5$	43 **Tc** $5s^2 4d^5$	44 **Ru** $5s^1 4d^7$	45 **Rh** $5s^1 4d^8$	46 **Pd** $4d^{10}$	47 **Ag** $5s^1 4d^{10}$	48 **Cd** $5s^2 4d^{10}$
57 **La** $6s^2 5d^1$	72 **Hf** $6s^2 5d^2$	73 **Ta** $6s^2 5d^3$	74 **W** $6s^2 5d^4$	75 **Re** $6s^2 5d^5$	76 **Os** $6s^2 5d^6$	77 **Ir** $6s^2 5d^7$	78 **Pt** $6s^1 5d^9$	79 **Au** $6s^1 5d^{10}$	80 **Hg** $6s^2 5d^{10}$
89 **Ac** $7s^2 6d^1$	104 **Unq** $7s^2 6d^2$	105 **Unp** $7s^2 6d^3$	106 **Unh** $7s^2 6d^4$	107 **Uns** $7s^2 6d^5$	108 **Uno** $7s^2 6d^6$	109 **Une** $7s^2 6d^7$			

Table 1: Partial Periodic Table of Transition Metals Showing Ground State Electronic Configurations The ground state electronic configuration of the transition metals are shown. Previous studies with Ti, V, and W studied ground states with two s electrons. The ground state of Mo has only one s electron.

Interest in transition metal chemistry has recently seen considerable increase, especially in gas phase oxidation reactions[1-8]. Of particular importance is the role transition metals play in catalysis, atmospheric chemistry, and chemical vapor deposition processes. For example, transition metals are used in the synthesis of various alcohols from CO and H_2,[9] in the oxidative dehydrogenation of ethane and other hydrocarbons,[10] and in promoting the catalytic destruction of organophophorus[11] and organosulfur[12] compounds. Additionally, transition metal compounds are important precursors in chemical vapor deposition processes.[13]

Some transition metals and their oxides can be found in the earth's atmosphere where they may influence atmospheric processes.[14] Transition metals enter the atmosphere either through meteor deterioration or by being transferred from the stacks of industrial plants. Because transition metals are such effective catalysts, the relatively small, but increasing, amount of transition metals in the atmosphere can have far reaching effects.

Transition metals have high spin multiplicities and a large number of low-lying electronic states. The many closely-spaced electronic states in these atoms can affect their reactivities. Three mechanisms for the oxidation of the transition metals by oxygen-containing molecules have been proposed: the abstraction, electron transfer, and s-p promotion models. These mechanisms describe possible processes by which metal monoxide products are formed.

1. Abstraction Model

The abstraction mechanism correlates transition metal reactivity with the electronic configuration of the transition metal atom. The reactivities of the ground and low-lying electronic states of the transition metal are expected to differ since the low-lying metal oxide product states have electron configurations which correlate to the s^1d^{n-1} states, but not to the s^2d^{n-2} states. Consequently, reaction barriers are expected for the s^2d^{n-2} states, but no such barriers are expected with the s^1d^{n-1} states. Experiments on Vanadium (V)[15] and Titanium (Ti)[2] indicate the s^2d^{n-2} configuration reacts at a much slower rate than the s^1d^{n-1} configuration in reactions involving several oxidants. Experiments like these are complicated by the fact that the s^1d^{n-1} configuration has additional

energy over the s^2d^{n-2} configuration. This may indicate that the increase in reaction rate may be an energy effect, and not caused by electronic configuration effects on reaction dynamics. However, the Mo + O_2 reaction indicated that the electron configuration plays a dominant role in the reaction kinetics.[16] For Mo reacting with O_2, the s^1d^5 a^7S_3 ground state is much more reactive than the excited s^2d^4 a^5D_J states even though the a^5D_J states have over 10,000 cm^{-1} more energy than the ground state.

The abstraction mechanism explains the reactivity differences between the ground and excited states of an individual transition metal. It fails, however, to predict the relative reactivity of different transition metals. Assuming that the reactivity relies solely on the energy difference between a ground state s^2d^{n-2} and the lowest s^1d^{n-1}, those transition metals with low lying s^1d^{n-1} states should react faster than transition metals with higher s^1d^{n-1} energy states. This assumption would predict that reactivities of Sc, Ti, and V with a single oxidant would increase in the order k(Sc) < k(Ti) < k(V). The actual ordering for the rate constants, even though they are similar, is k(Ti) < k(V) < k(Sc)[1,15,17,19]. These observations indicate that other factors are involved in the reactivity of transition metals.

2. Electron Transfer Model

The electron transfer mechanism suggests that the potential energy surfaces evolving from the ground and excited neutral transition metal atom states cross an ion-pair surface. The metal transfers an electron to the reactant. Therefore, the efficiency of the reaction is controlled by the distance

at which the electron is transferred. The reaction efficiency increases with decreasing ionization energy of the transition metal [IP(TM)], and by increasing electron affinity of the reactant gas [EA(OX)]. Because excited state atoms have lower effective ionization energies, the electron transfer can occur at a greater range, causing increased reactivity.

The electron transfer mechanism accounts for the ordering of the Ti, Sc, and V atoms with a particular reactant since the ionization potential of the atoms are IP(Sc) < IP(V) < IP(Ti). The mechanism also supports the difference in reactivities for the ground and excited states of V and Ti. It is, however, inconsistent with the reactivities of the different states of Mo with O_2. Furthermore, the electron transfer mechanism does not predict the relative rate constants for different oxidants. Comparison of reactions of a particular transition metal with different oxidants do not always directly correlate with the electron affinities of the reactants.[17]

3. S-P Promotion Method

The s-p promotion model states that reactivity is related to the sum of the ionization potential and the s-p promotion energy of the transition metal[18]. The s-p promotion energy is the energy required to promote a valence s electron to the lowest p orbital. This process allows partial sp hybridization. The minimum energy level barrier is obtained in the activated complex through resonance between an ionic and covalent structure. Chromium, which has an s-p promotion energy of 279 kJ mol^{-1} has a lower rate constant than Sc, Ti, or V with a promotion energy of 190 kJ mol^{-1}.

B. Objective

The objective of this research was to determine the rates of reactions of the Group 6 transition metal molybdenum (Mo) in the gas phase with oxygen-containing oxidants CO_2, NO, SO_2 and N_2O as a function of temperature and pressure. These reactions were studied to determine the fundamental factors affecting transition metal atom reactivities. By obtaining Arrhenius parameters for these reactions, geometric factors and energy barrier effects can be determined. Comparison of the parameters to those of other previously measured transition metal reactions may indicate the relationship between reactivity and the electronic states of the transition metals. In addition, comparison of Arrhenius parameters for different oxidants will indicate the effect the oxidant's physical properties have on reactivity.

The reactions investigated and their reaction enthalpies are:

$Mo + SO_2$	$\rightarrow$	$MoO + SO$	-46 kJ/mol	(1)
$Mo + CO_2$	$\rightarrow$	$MoO + CO$	-65 kJ/mol	(2)
$Mo + NO$	$\rightarrow$	$MoO + N$	34.4 kJ/mol	(3)
$Mo + N_2O$	$\rightarrow$	$MoO + N_2$	-430 kJ/mol	(4)

The reaction enthalpies given above are for the ground state molybdenum atoms. The reactions of excited molybdenum atoms with the oxidants can lead to physical quenching as well as chemical reaction. These two processes are discussed in the results.

II. Experimental

Pseudo-first order kinetic experiments ([Mo] << [oxidant]) were carried out in an apparatus with slowly flowing gas using a laser photodissociation/laser-induced fluorescence (LIF) technique. A schematic of the experimental setup is shown in Figure 1. The reaction cell was a stainless steel reducing 4-way cross (MDC, Part #405015) with attached sidearms and a sapphire window for optical viewing. The internal diameter of the chamber perpendicular to the sidearms (in the primary direction of gas flow) is 6.0 cm. The internal diameter of the chamber and sidearms along the laser beam axis is 3.5 cm. The reaction cell was contained in a commercial convection oven (Blue M, model 206F) for temperature dependence measurements. The oven had a thermocouple attached to its thermostat that measured temperature within a degree Kelvin. The temperature was checked with an additional, independent thermocouple that measured temperature within a hundredths of a degree Kelvin. The oven had holes drilled in it to allow for the exiting sidearms and the telescoping of the LIF signal to the PMT (Photomultiplier Tube).

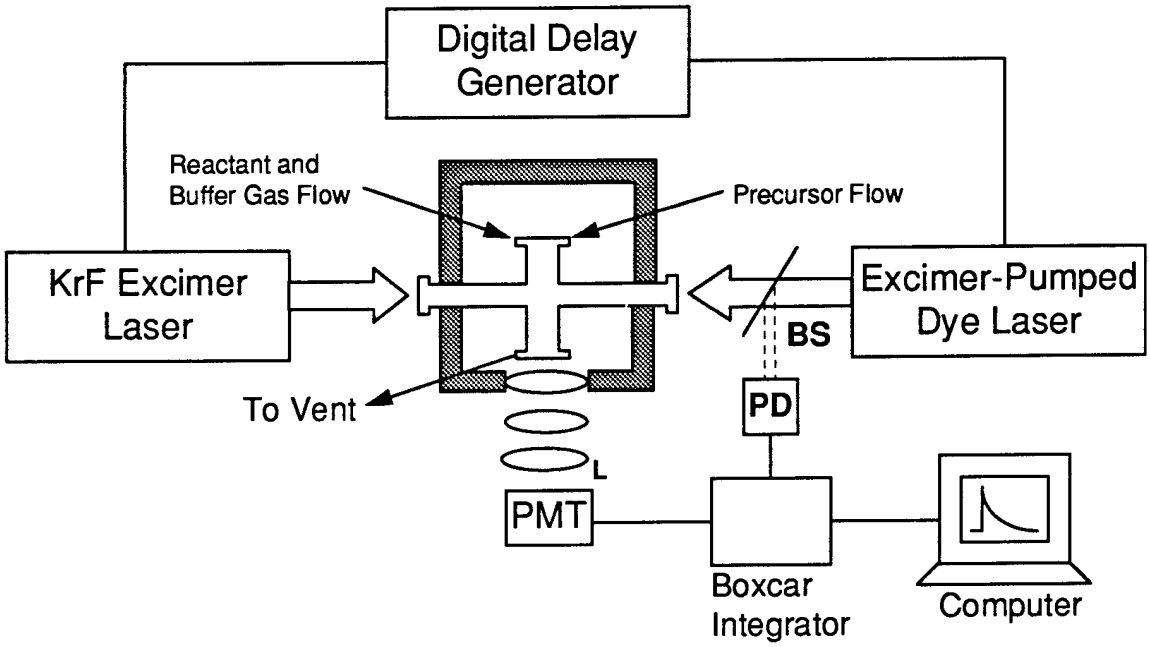

Figure 1: Schematic of Experimental Setup: Laser-Photodissociation / Laser Induced Fluorescence PMT = Photomultiplier Tube, L = Lens, BS = Beam Splitter, PD = Fast Photo Diode. The reaction cell (cross) is contained within a convection oven (shaded area). The pressure within the reaction cell is measured by a capacitance manometer. A pump is used to vent the gases.

Gas phase molybdenum atoms were produced from the excimer laser (Lambda Physics Lextra 200) photodissociation of molybdenum hexacarbonyl ($Mo(CO)_6$) and molybdenum tetrachloride ($MoCl_4$). Since $Mo(CO)_6$ decomposes at higher temperatures (500K), $MoCl_4$ had to be used exclusively at temperatures ranging from 500K to the limits of the apparatus (630K). $Mo(CO)_6$ was the preferred precursor, however, because it has a higher vapor pressure than $MoCl_4$. Photodissociation was accomplished at 248nm. This produced Mo atoms in all states studied. The kinetic results were independent of photodissociation laser fluence (50-400 mJ/cm^2) and Mo source.

Molybdenum atoms were detected via laser-induced fluorescence (LIF) utilizing the output of an excimer pumped dye laser (Lambda Physics Lextra 50 / ScanMate 2E). The dye laser excited the Mo in the states to be observed into an excited state (see Table 2). When these atoms relaxed, a characteristic fluorescence was observed (see Figure 2).

Mo Laser Induced Fluorescence

State	Excitation(nm)	Transition	Observation(nm)	Transition
a^5D_4	**603.07**	**$z^5P_3^o$ - a^5D_4**	**550**	**$z^5P_3^o$ - a^5S_2**
a^5D_3	428.86	$z^5F_4^o$ - a^5D_3	550	$z^5F_4^o$ - $a^5G_{4,5}$
a^5D_2	429.32	$z^5F_3^o$ - a^5D_2	550	$z^5F_3^o$ - $a^5G_{3,4}$
a^5D_1	429.21	$z^5F_2^o$ - a^5D_1	550	$z^5F_2^o$ - $a^5G_{2,3}$
a^5D_0	429.39	$z^5F_1^o$ - a^5D_0	550	$z^5F_1^o$ - a^5G_2
a^5S_2	**550.71**	**$z^5P_3^o$ - a^5S_2**	**600**	**$z^5P_3^o$ - a^5D_4**
a^7S_3	**390.26**	**$z^7P_2^o$ - a^7S_3**	**390**	**$z^7P_2^o$ - a^7S_3**

Table 2: Mo Laser Induced Fluorescence[19,20] Excitation by the dye laser at the given wavelength promotes Mo. Filters allowed observation of only the states of interest. Transitions of interest in this study are indicated in bold.

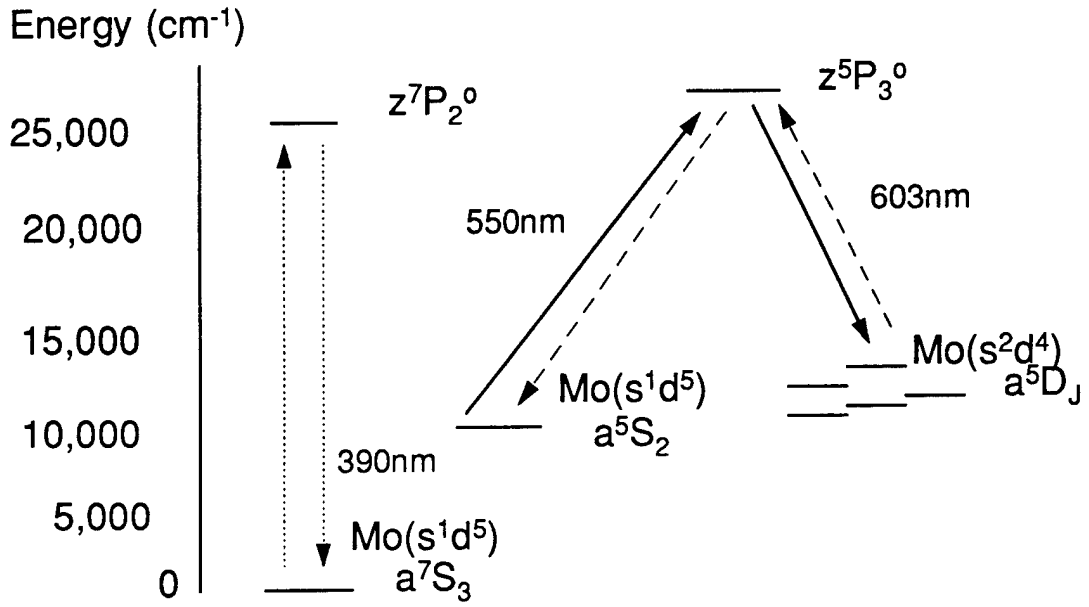

Figure 2: Energy Level Diagram for Mo Excitation and observation are done on different wavelengths for the excited states to minimize interference. This is not possible with the ground state because of the low probability of $z^7P_2^o$ relaxing to a different state.

For observation of the excited states, fluorescence was observed on a transition different than excitation so that fluorescence of other products of photodissociation, laser scatter and underlying emission would not interfere with the reading. This could not be done with the ground state, because the probability of transition to a different state was very low. LIF was monitored perpendicular to the counterpropagated laser beams with a three-lens telescope imaged through an iris into a photomultiplier tube (Hamamatsu R375). Interference filters were used to isolate the LIF. The PMT signal was dumped into a gated boxcar sampling module (Stanford Research Systems SR250). The boxcar was interfaced to a computer, and the digitized output was subsequently analyzed and stored by a computer. Real time viewing of the

photodissociation prompt emission and LIF signal were accomplished using a LeCroy Model 9360 digital oscilloscope.

The oxidizing agents were CO_2, SO_2, NO, and N_2O. The molybdenum precursor was entrained in a flow of argon gas. The diluted precursor, buffer gas, and oxidizing agent flowed through calibrated flow controllers and mass flow meters (MKS Types 1459C and 0258C, and Matheson models 8102 and 8202-1423) prior to admission to the reaction chamber. Each sidearm window was purged with a slow flow of buffer gas to prevent deposition of molybdenum and other photoproducts. Total flows were between 200 and 3500 sccm (standard cm^3/min). Pressures were measured with MKS Baratron manometers, and chamber temperatures were measured with a thermocouple. Typical precursor pressures were 1 to 150 μTorr.

The delay time between the photodissociation laser pulse and the dye laser probe was varied by using a digital delay generator (Stanford Research Systems DG535) controlled by a computer interfaced through a Stanford Research Systems SR245 computer interface. The trigger source for the oscilloscope and boxcar was scattered pump laser light incident upon a fast photodiode. LIF decay traces consisted of 200 - 400 points, and each point was averaged over 3 - 5 laser shots. The following reagents were used as received: $Mo(CO)_6$ (Aldrich, 98%), $MoCl_4$ (Aldrich, 99.3%), Ar (Potomac Airgas Inc., 99.998%), N_2O (MG Industries, 99.5%), NO (MG Industries, 99.0%), SO_2 (MG Industries, 99.98%), CO_2 (MG Industries, (Anaerobic) 99.98%).

III. Results

A. Data Analysis

The oxidation reaction (Mo + OX → MoO + X) is a bimolecular process, which relies on the concentration of both reactants to determine its rate.

$$\text{Rate} = k_{2nd}[Mo][OX] \tag{5}$$

However, during the experiment, there was an excess of oxidant ([OX] >> [Mo]), therefore, a pseudo first order rate law can be developed. Under pseudo-first order conditions in which no Mo production processes occur after the initial photodissociation event, the decrease in the [Mo] with time (see Figure 3) following the photodissociation laser pulse is given by:

$$\frac{-d[Mo]}{dt} = (k_{obs}[OX] + k_0)[Mo] \tag{6}$$

where k_{obs} is the observed rate constant due to oxidation at fixed buffer gas pressure, k_o is the depletion rate constant due to the reaction of Mo with precursor molecules and fragments and diffusion out of the detection zone.

For [OX] >> [Mo], Equation 6 can be solved to yield:

$$[Mo] = [Mo]_0 \exp(-t/\tau) \qquad (7)$$

where $1/\tau = k_{obs}[OX] + k_0$, [Mo] is the concentration of Mo at time t, and $[Mo]_0$ is the concentration of Mo at time 0. Equation 7 represents the pseudo first-order decay of Mo, and $1/\tau$ is the pseudo 1st order rate constant. The pseudo first order rate constants for a given reactant partial pressure and temperature can be obtained from the measured decrease in the metal atom LIF signal as a function of laser delay. The LIF signal is proportional to the Mo number density.

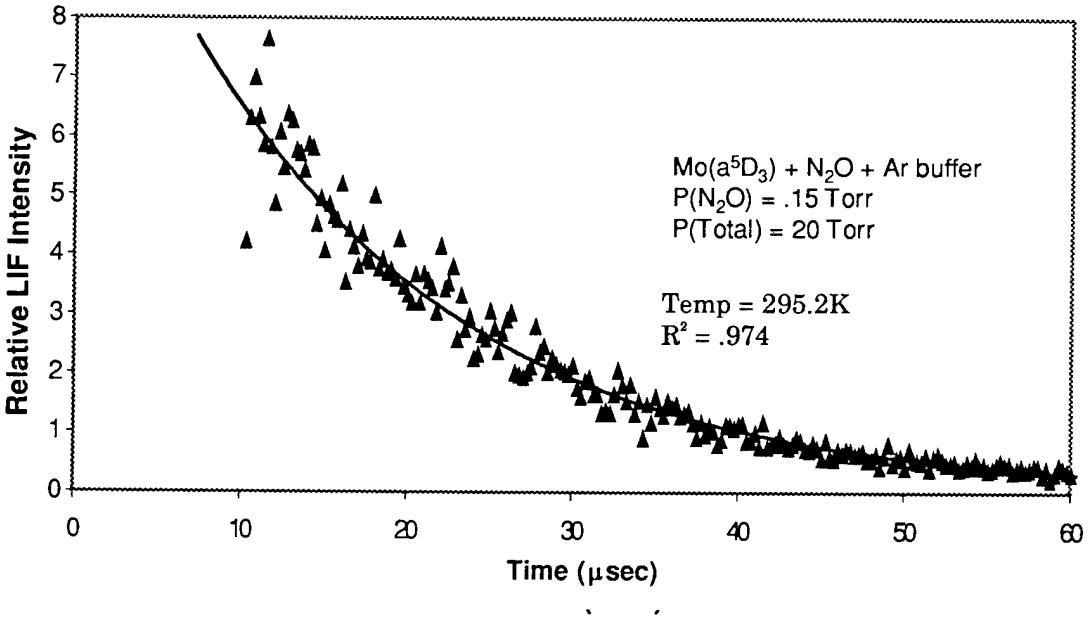

Figure 3: Typical Mo Decay Curve - Data is for Mo(a^5D_3) + N_2O.
Because the decay is a logarithmic function, the error is consistent throughout the time range. R^2 is for the straight line fit of ln(LIF) vs. Time.

Equation 7 can be represented as:

$$LIF = LIF_0 \exp(-t/\tau) \qquad (8)$$

where LIF_0 is the signal level in volts detected by the PMT immediately following the photodissociation laser pulse, t is the time from pulse in μsec, and τ is the time constant, also in μsec.

LIF decays which exhibited single exponential behavior were fitted using a least squares procedure to determine τ. Time constants covered a range of 5 to 300 μsec. The partial pressure of the reactants was adjusted to accommodate this, and insured uniform k readings. The slope of a plot of $1/\tau$ vs. oxidant pressure yields the observed rate constant k_{obs} (see Figure 4). Specific plots of $1/\tau$ vs. oxidant pressure can be found in the appendix.

Bimolecular rate constants for the different reactants were determined from the slope of the least-squares line fitting the first-order rate constants as a function of reactant gas pressure. The Arrhenius parameters were determined from the temperature dependence of the bimolecular rate constants (see Figure 5). A is a steric factor that helps describe how molecular geometry affects reaction. E_a is the activation energy of the reaction.

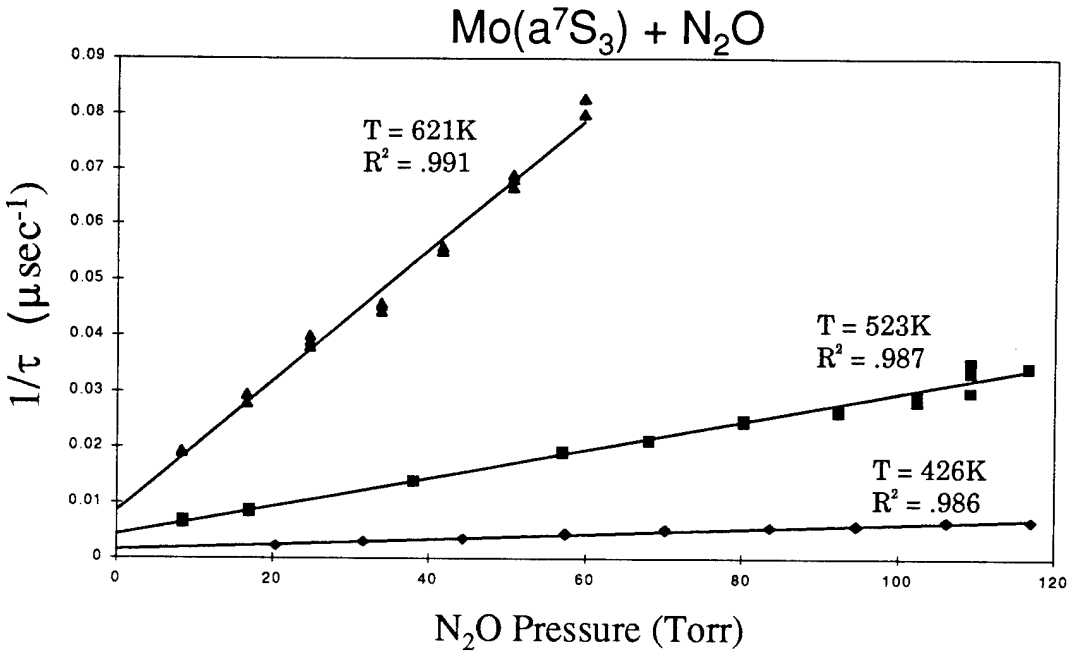

Figure 4: Plot of 1/τ vs. oxidant pressure k = (TR)/(Δτ ΔP), where T = Temperature and R = Gas Constant (62.36 L Torr K^{-1} mol^{-1}).

Figure 5 shows a typical Arrhenius plot and its interpretation. Because chemical reactions involve the rearrangement of bonds, most reactions don't occur without a certain amount of activation energy present. The activation energy, Ea, is obtained by multiplying the slope of the Arrhenius plot by R, the gas constant. The higher the reaction temperature, the more energy present that can be used as activation energy, and the faster the reaction will progress.

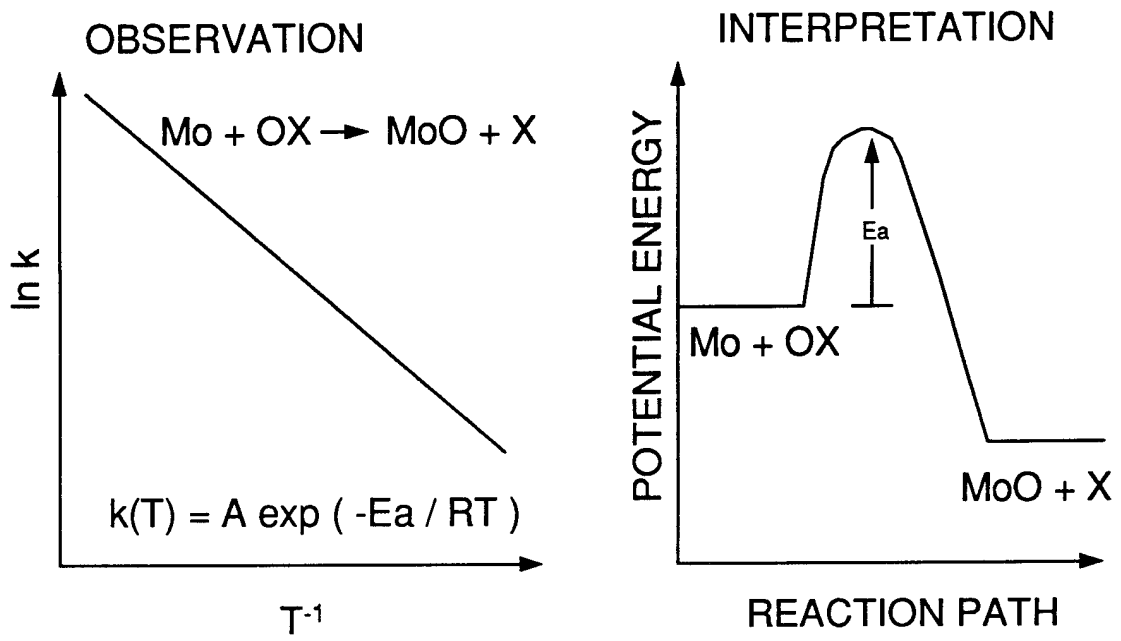

Figure 5: Interpretation of Arrhenius Plot Activation energy must be overcome for the reaction to progress. The higher the temperature of reaction, the more likely this energy barrier will be overcome and therefore the larger the reaction rate constant k.

The possibility exists for termolecular process involving the buffer gas for the reaction. This was only noted in the ground state reacting with NO (Mo + NO + Ar $\rightarrow$ MoNO + Ar). A third order rate law can be determined for this reaction, where Rate = k_{3rd}[Mo][NO][Ar]. The importance of termolecular processes was investigated by determining the bimolecular rate constant as a function of buffer gas pressure.

B. Discussion

There are four plausible mechanisms for the removal of atomic molybdenum in the presence of oxidant (OX = CO_2, N_2O, NO, SO_2). These mechanisms are:

$Mo + OX$	$\rightarrow$	$MoO + X$	(9)
$Mo + OX + Ar$	$\rightarrow$	$MoOX + Ar^*$	(10)
$Mo(a^5D_J) + M$	$\leftrightarrows$	$Mo(a^5D_{J'},a^7S_3,a^5S_2) + M^*$	(11)
$Mo(a^5S_2) + M$	$\leftrightarrows$	$Mo(a^7S_3, a^5D_J) + M^*$	(12)

M is either the oxidant, buffer gas, precursor, or precursor fragments, and the asterisk represents an atom or molecule with an energy different than its initial energy prior to collision.

The first reaction (9) is the bimolecular process where the Mo is directly oxidized by the oxidant.

The second reaction (10) is the termolecular association reaction. This reaction assumes that the Mo and the oxidant bound together to form an adduct. The excess energy from this adduct formation is passed along to the buffer gas (Ar). Because this reaction relies on the buffer gas, a pressure dependence should be noted in the reactions. The only reaction studied that showed a pressure dependence was the ground state Mo reacting with NO. A closer look at the complexation/abstraction reactions can provide some insight into the kinetics of the reaction.

The complexation/abstraction reaction scheme for the Mo and NO reaction is as follows:

$$Mo + NO \underset{k_{-1}}{\overset{k_1}{\rightleftarrows}} MoNO^* \quad (13)$$

$$MoNO^* \xrightarrow{k_2} MoO + N \quad (14)$$

$$MoNO^* + M \xrightarrow{k_3} MoNO + M^* \quad (15)$$

Equation 13 is the formation of an excited and unstable adduct. This adduct can be stabilized by direct abstraction, as shown in Equation 14, or by electronic quenching, as shown in Equation 15. The combination of these reactions would give an observed kinetic Equation as follows:

$$k_{obs} = \frac{k_1 \left(k_2 + k_3 [M]\right)}{k_{-1} + k_2 + k_3 [M]} \quad (16)$$

Equation 10 above assumes no abstraction method. Assuming abstraction does not occur allows simplification to the Lindemann-Hinshelwood expression:

$$k_{obs} = \frac{k_0 [M]}{1 + k_0 [M] / k_\infty} \quad (17)$$

In this equation, k_{obs} is the observed second-order rate constant, $k_0 = k_1 k_3 / k_{-1}$ is the limiting low-pressure third order rate constantat, $k_\infty = k_1$ is the limiting high-pressure second-order rate constant, and [M] is the buffer gas concentration.

The third and fourth reactions (11 and 12) are the removal or production of the Mo being studied through the use of electronic energy transfer. It is unlikely that the excited states of Mo convert to the ground state through

fluorescence because the transition is spin forbidden so would have a relatively long lifetime. However, electronic quenching is possible, where energy is transferred to surrounding particles, allowing the Mo to enter a new state. It is unlikely that the excited states are quenched to the ground state because the states are separated by 10000 cm^{-1}. However, transfer between states is possible. This transfer can be observed in a biexponential decay curve, where the first limb represents the loss of excited state Mo due to reaction, and the second represents the addition of Mo in the state being observed due to quenching of Mo in other excited states (see Figure 6). This was observed in the $Mo(a^5S_2) + N_2O$ and $Mo(a^5S_2) + CO_2$ reactions. Data that was shown to be biexponential was fit to the following equation.

$$LIF = A \cdot e^{-\frac{t}{\tau_1}} + B \cdot e^{-\frac{t}{\tau_2}} \quad (18)$$

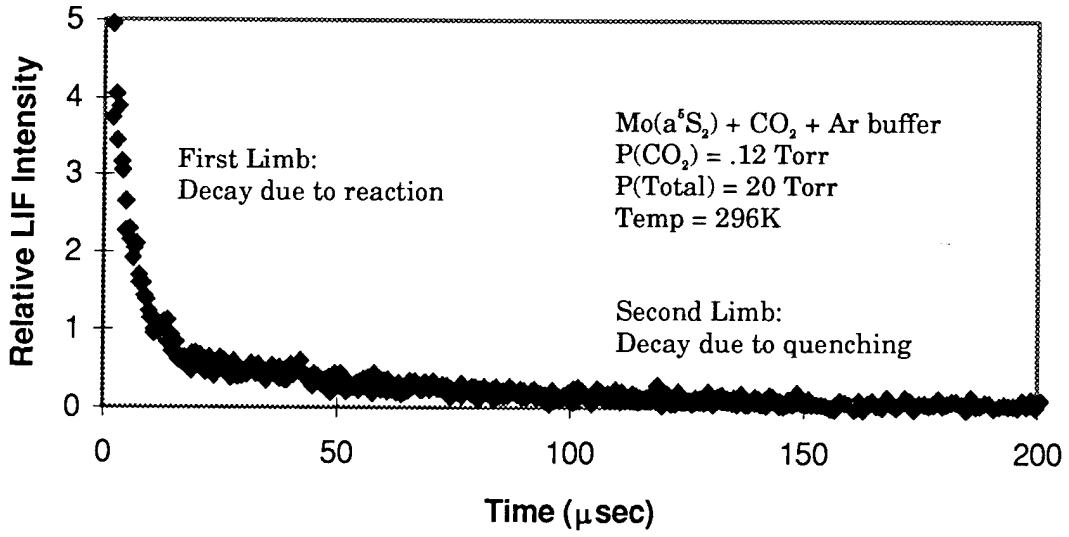

Figure 6: Biexponential Mo Decay Curve

C. Results

1. Reactions of Mo + N_2O

Reaction Rate Constants for Mo + N_2O (P_{tot} = 20 Torr)

State	Temp (K)	k(cm^3s^{-1})	A (cm^3s^{-1})	Ea (kJ mol^{-1})
a^7S_3 (s^1d^5)	400	1.0×10^{-15}	1.0×10^{-10}	38
(P=120 Torr)	426	2.1×10^{-15}		
	448	3.3×10^{-15}		
	480	6.6×10^{-15}		
	523	1.4×10^{-14}		
	561	3.0×10^{-14}		
	585	4.0×10^{-14}		
	606	5.9×10^{-14}		
	621	7.5×10^{-14}		
a^5S_2 (s^1d^5)	296	2.7×10^{-10}		
a^5D_4 (s^2d^4)	295	1.1×10^{-11}	4.8×10^{-11}	3.9
	398	1.3×10^{-11}		
	473	1.7×10^{-11}		
	621	2.5×10^{-11}		

Table 3: Reaction Rate Constants for Mo + N_2O

The reaction rate of Mo(a^7S_3) with N_2O is very small. Even though data were collected at an increased pressure of 120 Torr, reaction rates at room temperature were all less than 7×10^{-14} cm^3s^{-1}, which was about the slowest that the apparatus could measure with any reliability. The slow reaction at room temperature and the high activation energy shown in Table 3 indicate that there are significant barriers to the reaction. The Arrhenius plot in Figure 7 shows that the activation energy of the ground state reaction is 38 kJ mol^{-1}.

Biexponential behavior was noted in the Mo(a^5S_2) reaction. The fast reaction observed is the reaction of interest (see Figure 6). The reaction rate determined from the first limb is near the gas kinetic rate, therefore higher

temperature observation would not have provided any new information. As other states are quenched to a^5S_2, they are observed as they react, as seen in the second limb of the reaction.

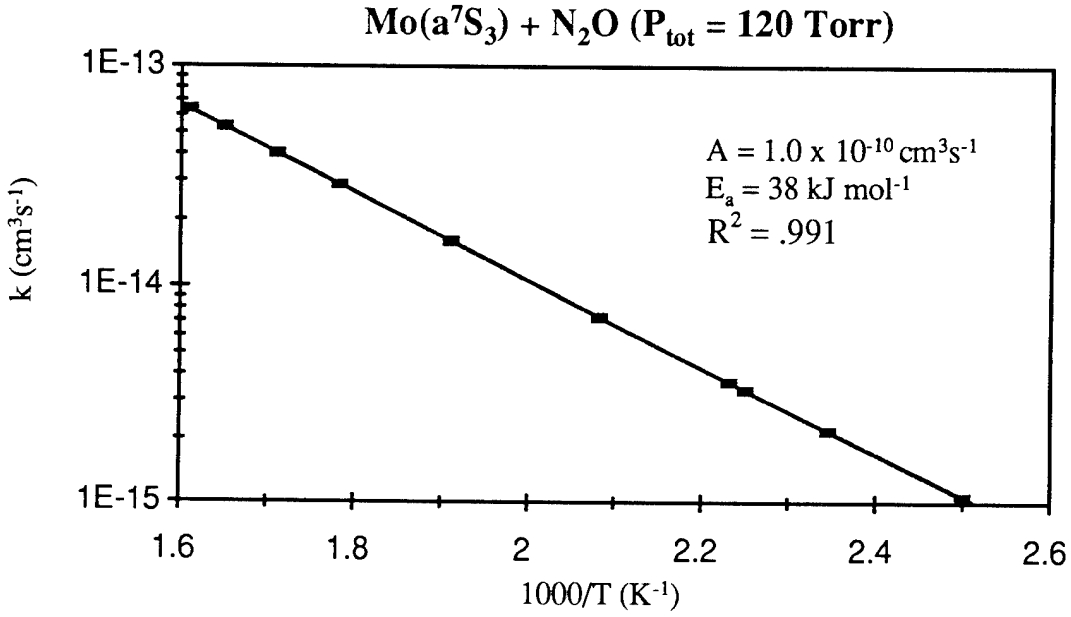

Figure 7: Arrhenius Plot of $Mo(a^7S_3) + N_2O$

Examination of the molecular orbitals of the ground state reactants and products indicates that an oxidation of Mo by N_2O is spin-forbidden.

$$Mo(a^7S_3) + N_2O(^1\Sigma^+) \rightarrow \quad MoO(^5\Pi) + N_2(^1\Sigma^+) \qquad (19)$$

The reactivity of the excited state of Mo follows the hypothesis that transition metals with a single electron in the s orbital will react faster than those with two electrons in the s orbital. $Mo(a^5S_2)$, which has a s^1d^5 configuration reacts 25 times faster than $Mo(a^5D_4)$ which has a s^2d^4 configuration.

2. Reactions of Mo + CO_2

Reaction Rate Constants for Mo + CO_2 (P_{tot} = 20 Torr)

State	Temp (K)	k(cm^3s^{-1})	A (cm^3s^{-1})	Ea (kJ mol^{-1})
a^7S_3 (s^1d^5)	296	$<1 \times 10^{-15}$		
(P=120 Torr)	430	$<1 \times 10^{-15}$		
	620	$<1 \times 10^{-15}$		
a^5S_2 (s^1d^5)	296	7.1×10^{-11}		
a^5D_4 (s^2d^4)	296	3.1×10^{-12}	3.7×10^{-11}	6.2
	398	5.9×10^{-12}		
	473	6.7×10^{-12}		
	621	1.2×10^{-11}		

Table 4: Reaction Rate Constants for Mo + CO_2

The reactivities of Mo with CO_2 are found in Table 4. The ground state of Mo reacting with CO_2 was found to be very slow, even at a higher total pressure. This is due, again, to a spin forbidden reaction:

$$Mo(a^7S_3) + CO_2(^1\Sigma^+) \rightarrow MoO(^5\Pi) + CO(^1\Sigma^+) \qquad (20)$$

The excited states, however, react in accordance with the hypothesis. $Mo(a^5S_2)$, which has a s^1d^5 configuration which reacts 23 times faster than $Mo(a^5D_4)$ which has a s^2d^4 configuration.

Again, biexponential behavior was noted in the $Mo(a^5S_2)$ reaction. The fast reaction observed is the reaction of interest. As other states are quenched to a^5S_2, they are observed as they react.

3. Reactions of Mo + SO_2

Reaction Rate Constants for Mo + SO_2 (P_{tot} = 20 Torr)

State	Temp (K)	k($cm^3 s^{-1}$)
a^7S_3 (s^1d^5)	300	1.9×10^{-10}
a^5S_2 (s^1d^5)	299	3.3×10^{-10}
a^5D_4 (s^2d^4)	298	3.0×10^{-10}

Table 5: Reaction Rate Constants for Mo + SO_2

All the removal rate constants for the reactions with SO_2 are near the gas kinetic rate (see Table 5). This means that as soon as the reactants collide, they react with little or no activation energy required. The reaction is spin allowed.

$$Mo(a^7S_3) + SO_2(^1A_1) \rightarrow MoO(^5\Pi) + SO(^3\Sigma^-) \qquad (21)$$

No barriers to these reactions appear to exist. Therefore electronic configuration does not appear to influence the reactivity. A possible explanation for this is that there is electronic quenching between the excited electronic states.

4. Reactions of Mo + NO

Reaction Rate Constants for Mo + NO (P_{tot} = 20 Torr)				
State	T(K)	k(cm^3s^{-1})	A(cm^3s^{-1})	Ea(kJ mol^{-1})
a^7S_3 (s^1d^5)	297	9.1×10^{-12}		
	336	8.6×10^{-12}		
	376	7.7×10^{-12}		
	413	7.1×10^{-12}		
	621	2.4×10^{-12}		
a^5S_2 (s^1d^5)	298	3.3×10^{-11}	1.6×10^{-10}	4.0
	373	4.2×10^{-11}		
	450	5.3×10^{-11}		
	621	7.6×10^{-11}		
a^5D_4 (s^2d^4)	295	3.9×10^{-11}	1.2×10^{-11}	3.0
	373	4.2×10^{-11}		
	413	4.7×10^{-11}		
	446	4.8×10^{-11}		
	621	7.6×10^{-11}		

Table 6: Reaction Rate Constants for Mo + NO

The bimolecular process for the reaction of Mo(a^7S_3) with NO to form MoO is endothermic by 34.4 kJ/mole. Table 7 shows that the reaction is pressure dependent. This pressure dependent data can be fit to the Lindemann-Hinshelwood expression, as shown in Figure 8. For the pressure data taken at 298K, the third order $k_0 = 1.7 \times 10^{-29}$ cm^6s^{-1}, whereas the second order $k_\infty = 4.7 \times 10^{-11}$. For the 450K data, $k_0 = 1.1 \times 10^{-29}$, and $k_\infty = 5.3 \times 10^{-11}$ cm^3s^{-1}. The reaction appears to show some temperature dependence, but it does not exhibit Arrhenius behavior. At higher temperatures, the reaction rate decreased, indicating that the adduct falls apart at higher temperatures.

Using Table 6, it can be seen that the kinetic properties of Mo(a^5S_2) + NO and Mo(a^5D_4) + NO are very similar. A possible explanation of this could be electronic quenching between the excited states. (See Equations 11-12)

Measured Reaction Rate Constants for $Mo(a^7S_3) + NO$

Pressure (Torr)	$k(cm^3s^{-1})$ @T=296K	$k(cm^3s^{-1})$ @T=450K
10	5.9×10^{-12}	3.4×10^{-12}
20	9.6×10^{-12}	6.0×10^{-12}
35	1.5×10^{-11}	6.9×10^{-12}
50	1.8×10^{-11}	1.0×10^{-11}
75	2.2×10^{-11}	1.4×10^{-11}
100	2.7×10^{-11}	1.6×10^{-11}
150	2.8×10^{-11}	2.2×10^{-11}
200	3.1×10^{-11}	2.2×10^{-11}
250	3.6×10^{-11}	2.6×10^{-11}
300	3.8×10^{-11}	3.5×10^{-11}
400	4.2×10^{-11}	3.5×10^{-11}
600	4.4×10^{-11}	4.7×10^{-11}

Table 7: Pressure Dependence of Reaction Rate Constants for $Mo(a^7S_3) + NO$

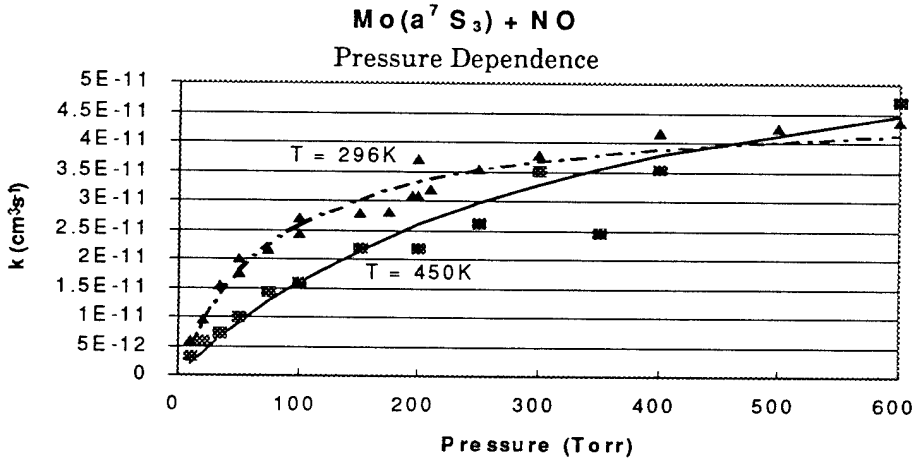

Figure 8: Pressure Dependence of $Mo(a^7S_3) + NO$

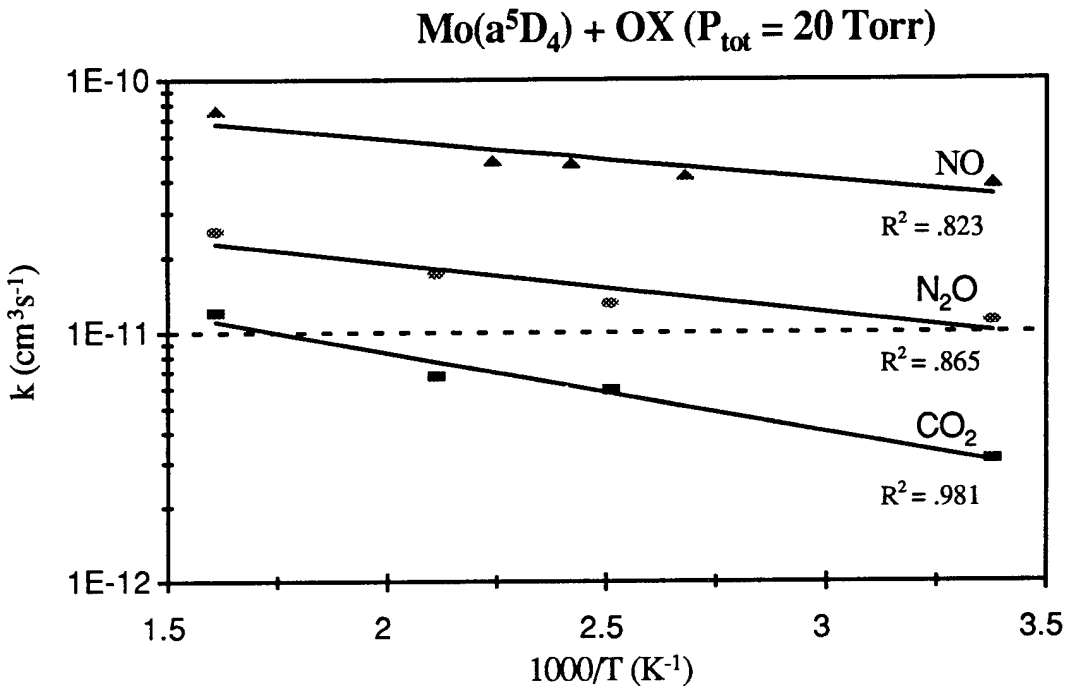

Figure 9: Arrhenius Plot of Mo(a^5D_4) + OX

D. Summary

The removal rate constants for Mo(a^5S_2) with CO_2 and N_2O (Table 3-4) are significantly faster than the removal rate constants of the a^5D_4 state (Table 3-4). This supports the hypothesis that the rate of reaction depends on the s^1d^5 vs. s^2d^4 configuration. However, electronic configuration is not the most important thing to look at when determining how fast a reaction will progress. The experimental data showed that a few other considerations have to be accounted for first. The removal rate constants for the s^1d^5 configuration of Mo(a^7S_3) with CO_2 and N_2O are slow because they are spin forbidden. Because of the thermodynamic barrier in the Mo + NO reaction, the reaction rate constants are not dependent on the electronic configuration of the valence shell. Additionally, the effects of electronic quenching between excited states need to be understood, as proven by the inconclusive NO and SO_3 results.

Therefore, the most important consideration when looking at the oxidation of a transition metal is if the reaction is spin allowed. If the reaction is not spin allowed, it will take a very long time to react and will require a lot of activation energy.

The second consideration is the thermodynamics of the reaction. If the oxidation will not produce stable products, the direct oxidation will not occur. Instead, a different reaction path (e.g. adduct formation or electronic quenching) will be followed.

Finally, the mechanism of the reaction should be examined. Knowing how the electrons interact, be it by electron transfer, abstraction, or s-p interaction, can give clues on which reactions are more favorable. The kinetic information gathered can be used for molecular orbital calculations of the transition states.

Further research would give a broader understanding of how electronic configuration affects the reaction rates of transition metals. Study of platinum (Pt s^1d^9) and palladium (Pd d^{10}), both well known catalysts, would give expensive, but informative data.

REFERENCES

[1] Ritter, D.; Weisshaar, J.C., *J. Phys. Chem.* **1989**, *93*, 1576.

[2] Clemmer, D.E.; Honma, K.; Koyano, I., *J. Phys. Chem.* **1993**, *97*, 11480.

[3] Mitchell, S.A.; Hackett, P.A. *J. Phys. Chem.*. **1990**, *93*, 7822.

[4] Parnis, J.M.; Mitchell, S.A.; Hackett, P.A. *J. Phys. Chem.* **1990**, *94*, 8152.

[5] Brown, C.E.; Mitchell, S.A.; Hackett, P.A. *J. Phys. Chem.* **1991**, *95*, 1062.

[6] Lian, L.; Mitchell, S.A.; Rayner, D.M. *J. Phys. Chem.* **1994**, *98*, 11637.

[7] Vinckier, C.; Corthouts, J.; De Jaegere, S.J. *Chem. Soc., Faraday Trans. 2.* **1988**, *84*, 1951.

[8] Honma, K.; Nakamura, M.; Clemmer, D.E.; Koyano, I. *J. Phys. Chem* . **1994**, *98*, 13286.

[9] Maramatsu, A.; Tatsumi, T.; Tominaga, H. *J. Phys. Chem.* **1992**, *96*, 1334.

[10] Le Bars, J.; Vedrine, J.C.; Auroux, A.; Pommier, B.; Pajonk, G.M. *J. Phys Chem.* **1992**, *96*, 2217.

[11] Guo, X.; Yoshinobu, J.; Yates, Jr., J.T. *J. Phys. Chem.* **1990**, *94*, 6839.

[12] Huntley, D.R. *J. Phys. Chem.* **1992**, *96*, 4551.

[13] Eden, J.G. *Photochemical Vapor Deposition;* Wiley: New York, **1992.**

[14] Brown, T.L. *Chem. Rev.* **1973**, *73*, 645.

[15] McClean, R.E., Pasternack, L., *J. Phys. Chem* **1992**, *96*, 9828.

[16] Campbell, M.L.; McClean, R.E.; Harter, J.S.S *Chem. Phys. Lett.* **1995**, *235*, 497.

[17] Campbell, M.L., McClean, R.E., *J. Phys. Chem.* **1993**, *97*, 7942.

[18] Fontijn, A., Futerko, P.M. *J. Chem. Phys.* **1991**, *95*, 8065.

[19] Moore, C.E., Atomic energy levels as derived from the analysis of optical spectra, NSRDS-NBS Circular No. 35 (US GPPO, Washington, 1971).

[20] Whaling, W.; Hanaford, P.; Lowe, R.M.; Biemont, E.; Grevesse, N. *J. Quantum Spectry. Radiative Transfer* **1984**, *32*, 69.

Appendix

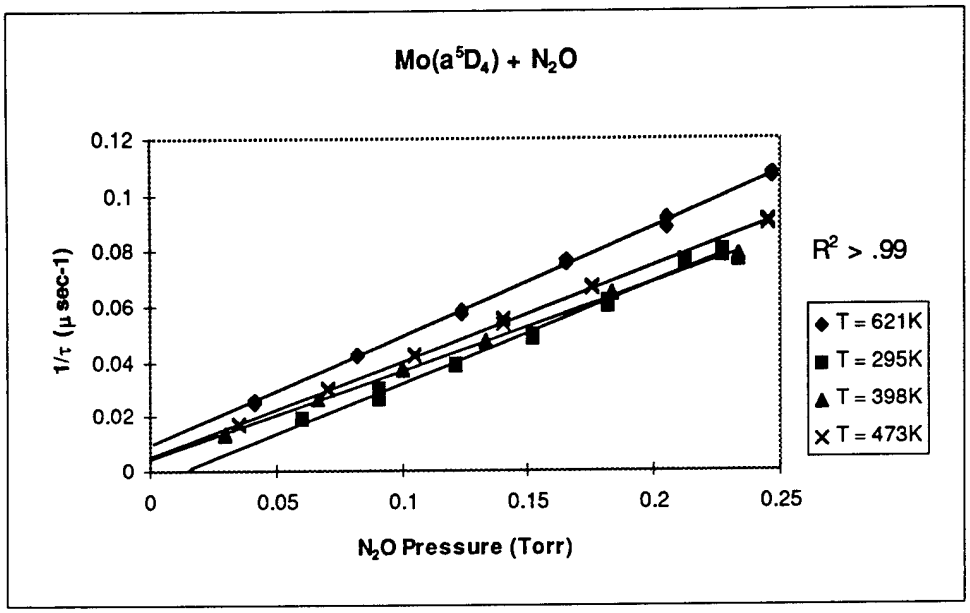
Mo(a5D4) + N2O
0.12
0.1
0.08
0.06
0.04
0.02
0
1/τ (μ sec-1)
0
0.05
0.1
0.15
0.2
0.25
N2O Pressure (Torr)
R2 > .99
T = 621K
T = 295K
T = 398K
T = 473K

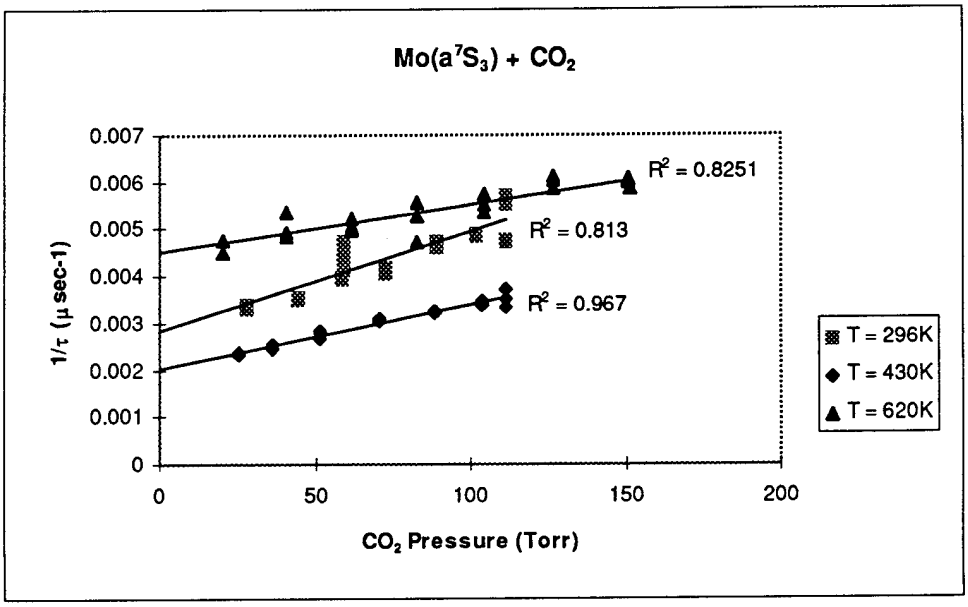
Mo(a7S3) + CO2
0.007
0.006
0.005
0.004
0.003
0.002
0.001
0
1/τ (μ sec-1)
0
50
100
150
200
CO2 Pressure (Torr)
R2 = 0.8251
R2 = 0.813
R2 = 0.967
T = 296K
T = 430K
T = 620K

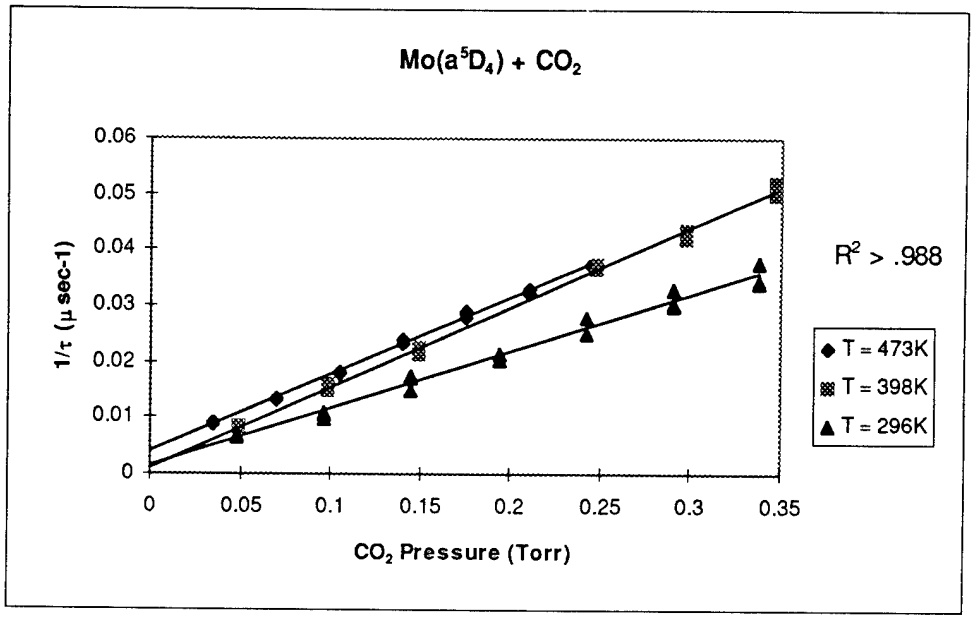
Mo(a5D4) + CO2
0.06
0.05
0.04
0.03
0.02
0.01
0
1/τ (μ sec-1)
0
0.05
0.1
0.15
0.2
0.25
0.3
0.35
CO2 Pressure (Torr)
R2 > .988
T = 473K
T = 398K
T = 296K

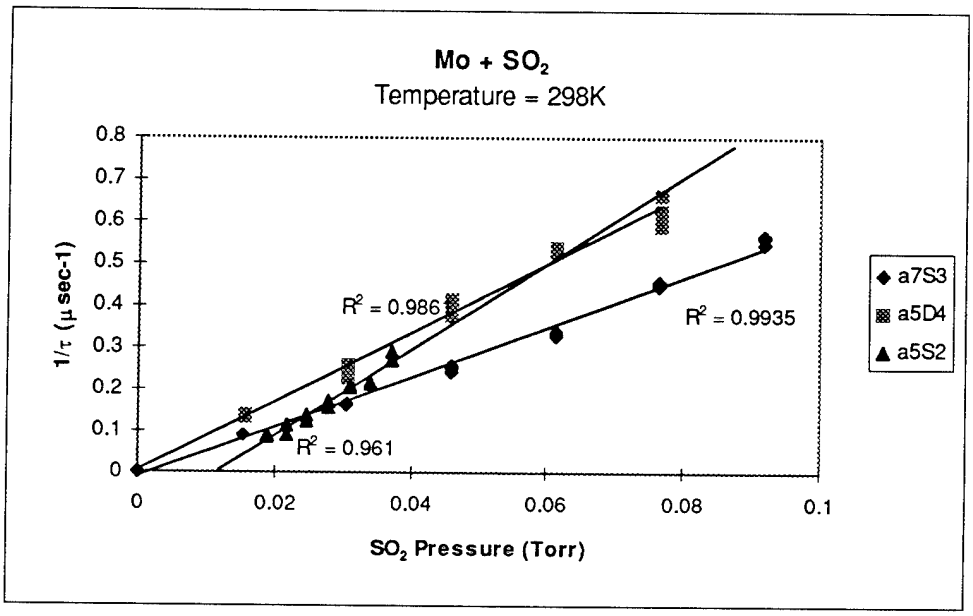
Mo + SO2
Temperature = 298K
0.8
0.7
0.6
0.5
0.4
0.3
0.2
0.1
0
1/τ (μ sec-1)
R2 = 0.986
R2 = 0.9935
R2 = 0.961
0
0.02
0.04
0.06
0.08
0.1
SO2 Pressure (Torr)
a7S3
a5D4
a5S2

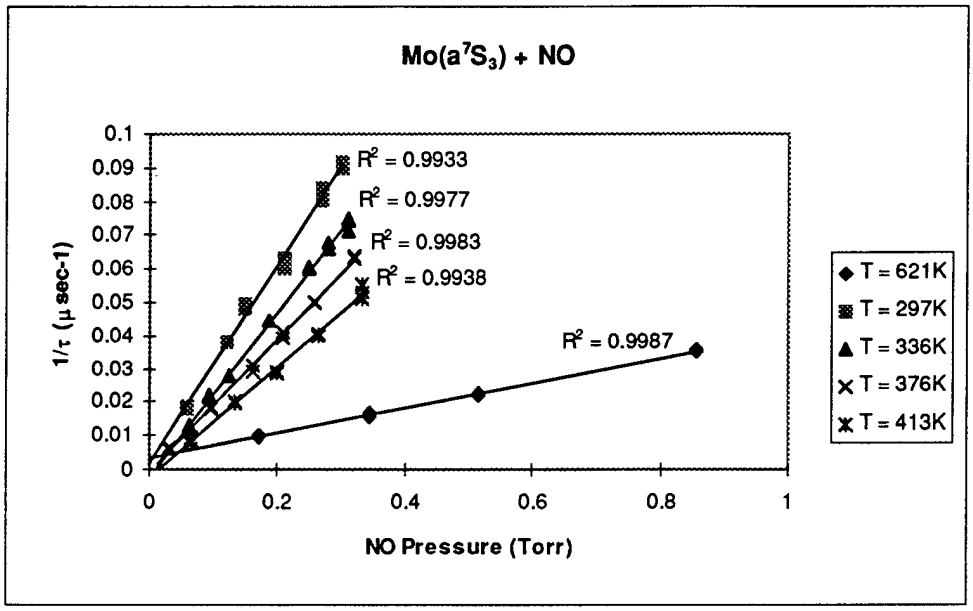
Mo(a7S3) + NO
1/τ (μ sec-1)
0.1
0.09
0.08
0.07
0.06
0.05
0.04
0.03
0.02
0.01
0
R2 = 0.9933
R2 = 0.9977
R2 = 0.9983
R2 = 0.9938
R2 = 0.9987
0
0.2
0.4
0.6
0.8
1
NO Pressure (Torr)
T = 621K
T = 297K
T = 336K
T = 376K
T = 413K

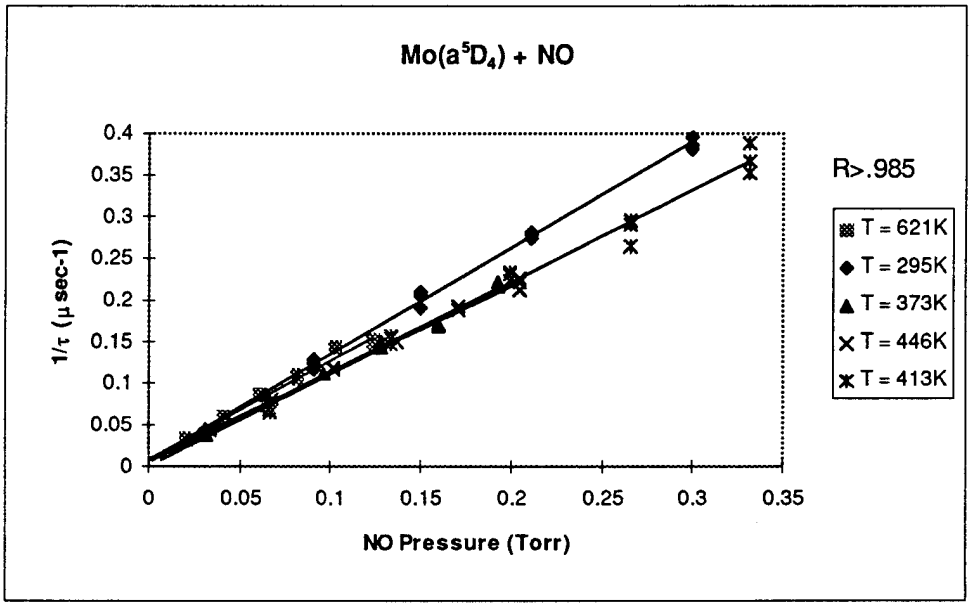
Mo(a5D4) + NO
1/τ (μ sec-1)
0.4
0.35
0.3
0.25
0.2
0.15
0.1
0.05
0
0
0.05
0.1
0.15
0.2
0.25
0.3
0.35
NO Pressure (Torr)
R>.985
T = 621K
T = 295K
T = 373K
T = 446K
T = 413K